# Multiscale Free Energy Simulations: An Efficient Method for Connecting Classical MD Simulations to QM or QM/MM Free Energies Using Non-Boltzmann Bennett Reweighting Schemes

Gerhard König,[†] Phillip S. Hudson,[‡] Stefan Boresch,*[,§] and H. Lee Woodcock*[,‡]

[†]Laboratory of Computational Biology, National Heart Lung and Blood Institute, National Institutes of Health, Bethesda, Maryland 20892, United States

[‡]Department of Chemistry, University of South Florida, 4202 E. Fowler Avenue, CHE205, Tampa, Florida 33620-5250, United States

[§]Department of Computational Biological Chemistry, Faculty of Chemistry, University of Vienna, Währingerstraße 17, A-1090 Vienna, Austria
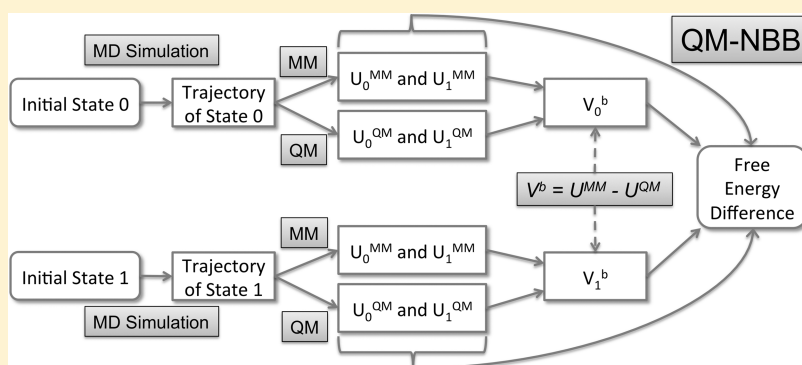
ABSTRACT: The reliability of free energy simulations (FES) is limited by two factors: (a) the need for correct sampling and (b) the accuracy of the computational method employed. Classical methods (e.g., force fields) are typically used for FES and present a myriad of challenges, with parametrization being a principle one. On the other hand, parameter-free quantum mechanical (QM) methods tend to be too computationally expensive for adequate sampling. One widely used approach is a combination of methods, where the free energy difference between the two end states is computed by, e.g., molecular mechanics (MM), and the end states are corrected by more accurate methods, such as QM or hybrid QM/MM techniques. Here we report two new approaches that significantly improve the aforementioned scheme; with a focus on how to compute corrections between, e.g., the MM and the more accurate QM calculations. First, a molecular dynamics trajectory that properly samples relevant conformational degrees of freedom is generated. Next, potential energies of each trajectory frame are generated with a QM or QM/MM Hamiltonian. Free energy differences are then calculated based on the QM or QM/MM energies using either a non-Boltzmann Bennett approach (QM-NBB) or non-Boltzmann free energy perturbation (NB-FEP). Both approaches are applied to calculate relative and absolute solvation free energies in explicit and implicit solvent environments. Solvation free energy differences (relative and absolute) between ethane and methanol in explicit solvent are used as the initial test case for QM-NBB. Next, implicit solvent methods are employed in conjunction with both QM-NBB and NB-FEP to compute absolute solvation free energies for 21 compounds. These compounds range from small molecules such as ethane and methanol to fairly large, flexible solutes, such as triacetyl glycerol. Several technical aspects were investigated. Ultimately some best practices are suggested for improving methods that seek to connect MM to QM (or QM/MM) levels of theory in FES.

1. INTRODUCTION

Free energy simulations (FES) have become an indispensable tool in biophysics. Application of FES has become amazingly broad and includes free energy calculations of ligand binding,[1−6] solvation,[7,8] protein mutation,[9,10] pK_a,[11−15] redox potentials,[16,17] and more. Although the application of FES has become more routine, there are still two fundamental prerequisites: the *accurate description of inter- and intramolecular interactions*, and *adequate sampling of all relevant conformational degrees of freedom*.[18,19] For example, the recent SAMPL blind prediction competitions[20−28] have highlighted the need for

proper treatment of polarization, high quality charges, and bonded parameters, as well as the necessity of extensive conformational sampling.

One logical approach to improving the treatment of inter- and intramolecular interactions in FES is to move beyond molecular mechanical (MM) methods; in fact, the application of quantum mechanical (QM) and QM/MM techniques in FES is now the source of intense interest.[29−42] However, the

requirement for adequate conformational sampling presents a major challenge. Typically, free energy differences between two states are computed via a series of molecular dynamics (MD) or Monte Carlo (MC) simulations, each consisting of typically 10^5-10^7 energy and force calculations. While this level of computational effort is routine in MM simulations, it quickly becomes prohibitive if ab initio or density functional theory (DFT) is required. Semiempirical QM (SQM) or empirical valence bond (EVB) approaches can reduce the computational effort;[43−50] however, these come with well-known accuracy limitations.[51−54] [For the remainder of this manuscript, we will use the following abbreviations: QM/MM refers to ab initio or DFT (e.g., HF, DFT, MP2, etc.) based Hamiltonians coupled to MM; SQM/MM indicates semiempirical QM (e.g., SCC-DFTB, AM1, PM3, etc.) based Hamiltonians coupled to MM; and (S)QM/MM denotes the use of either semiempirical or EVB methods. For convenience, we subsume all of the these approaches as "QM" since the FES methods described herein are independent of Hamiltonian.] Highlighting these weaknesses is an active resurgence in the development of improved SQM potentials,[51,55−57] but higher level ab initio/DFT methods remain essential where accurate results are desired and/or unique chemical environments encountered.[58−61]

So-called *indirect* schemes for FES employing QM Hamiltonians remove some of the contradictory requirements of accuracy and sufficient sampling. This technique was largely pioneered by Gao and co-workers and Warshel and co-workers,[43−47] with generalizations and extensions made by numerous others.[48,62−70] The basic premise behind indirect FES is the use of a thermodynamic cycle to calculate the free energy between two states, 0 and 1, at a *high* level of theory in three steps: i.e.,

$$\Delta A(0_{\text{high}} \rightarrow 1_{\text{high}}) = -\Delta A(0_{\text{low}} \rightarrow 0_{\text{high}})$$
$$+ \Delta A(0_{\text{low}} \rightarrow 1_{\text{low}}) + \Delta A(1_{\text{low}} \rightarrow 1_{\text{high}}) \quad (1)$$

Here, *high* denotes the use of an accurate method, typically QM or QM/MM, which in general is too expensive for large

Scheme 1. Typical Thermodynamic Cycle Used in *Indirect* Free Energy Calculations
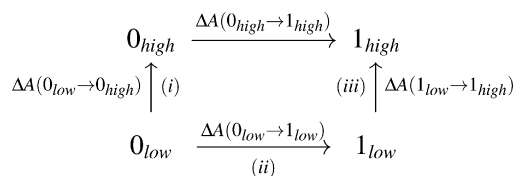
scale MD simulations. The label *low*, on the other hand, denotes a level of theory at which MD simulations can be carried out easily; this could be plain MM or SQM/MM. Thus, expensive QM calculations are only required in steps (i) and (iii) of the thermodynamic cycle, whereas the transformation (ii) $0_{\text{low}} \rightarrow 1_{\text{low}}$ is carried out at, e.g., the MM level. Aside from lowering the computational cost, this makes it possible to use specialized techniques, such as soft-core potentials, to avoid the so-called van der Waals end point problem.[71,72]

Indirect approaches reduce the computational complexity of QM FES significantly since in practice no QM MD simulations are carried out at all. The free energy differences $\Delta A(0_{\text{low}} \rightarrow 0_{\text{high}})$ and $\Delta A(1_{\text{low}} \rightarrow 1_{\text{high}})$ are typically computed by free energy perturbation (FEP, also known as Thermodynamic

Perturbation or Zwanzig's exponential formula),[73] using only a subset of configurations at the MM end states, for which the QM energy is computed. However, if the potential energy surfaces of the MM and the QM description of states 0 and 1 are significantly different, configurations sampled by MM will not be representative of those at QM. In such situations FEP does not converge and the free energy differences for steps (i) and (iii) above will be inaccurate and "noisy". Yang and co-workers,[74] as well as Rod and Ryde,[64,65] circumvented the problem by "freezing" the QM region [*QM region* denotes those atoms which at the high level of theory are computed by ab initio or DFT] during the pure MM calculations; these fixed atoms interact with the MM atoms through assigned electrostatic potential (ESP) derived point charges. The dual-level strategy for QM/MM calculations by Moliner, Tuñón, et al. provides an alternative to frozen QM regions; however, while the method was used in computations of kinetic isotope effects, it has not been used in "traditional" QM/MM free energy simulations.[75,76]

Warshel and co-workers have criticized the use of frozen QM regions for quite some time;[77,78] clearly, any entropic contributions from that region will not be accounted for. To overcome the large differences between the MM and QM potential energy surfaces, Warshel and co-workers replace the MM description with an EVB one that is specifically parametrized to reproduce the QM target states.[42,77] Recently, Heimdal and Ryde also pointed out the limitations of frozen QM regions.[79] However, despite using either specially parametrized force fields or a SQM/MM description of the quantum region, the FEP steps connecting the low and high levels of theory (i, iii) converged poorly, or at least very slowly, when a flexible QM region was employed. Recent work by Essex and co-workers avoided convergence problems of FEP by inserting differences in interaction energy rather than total energy differences into the FEP formula.[80,81]

In classical FES it has been known for quite some time[82−85] that FEP is much less efficient than Bennett's acceptance ratio (BAR) method.[86] Specifically, BAR can often be used to compute a free energy difference in a single step where other methods, such as FEP or thermodynamic integration (TI),[87] require intermediate steps.[88] FEP and BAR are examples of what has been referred to as one- and two-sided methods to compute free energy differences, respectively.[89] Two-sided methods require simulations at both end points; i.e., in the present context simulations with both the MM *and* the QM Hamiltonian. Since calculations with the latter are prohibitively expensive, BAR so far seems not to be used in QM FES. In some cases, Warshel and co-workers employed another two-sided method, linear response approximation.[41,42,90]

It follows from the overview just given that an ideal (indirect) QM FES employs a flexible QM region and computes the free energy differences for steps (i) and (iii) above accurately and precisely by employing a BAR-like approach. One possible way to avoid the costs of directly simulating the QM end states, as required for BAR, is to generate them "virtually" from MM or SQM/MM simulations. Recently, it was demonstrated how to conduct such calculations by regarding low level simulations as a special case of high level simulations in the presence of an *unusual* biasing potential. By accounting for those biasing potentials, it is possible to obtain free energy differences between the virtual high level end states; an approach referred to as Non-Boltzmann-Bennett (NBB).[91] In ref 91, the utility of this approach was illustrated for two

classical implicit solvent models with significantly different computational costs, saving about a factor of 10 in computer time compared to using the more accurate, but expensive, model throughout. Herein, we describe how NBB can be combined with an indirect QM FES approach without actually having to carry out expensive QM simulations. As in standard indirect schemes, it is enough to recompute energies of selected configurations sampled with a low level of theory, e.g., MM, at the desired QM level. Since this is a postprocessing step and individual configurations are independent of each other, these calculations are embarrassingly parallel.

In the current work, technical details of this new approach (i.e., QM-NBB) are presented with particular emphasis on methodological and technical aspects of FES methods that connect MM and QM levels of theory. In addition to utilizing NBB in indirect QM FES schemes, we also extend FEP to incorporate unusual biasing potentials; this results in a formulation of FEP better suited to connecting two levels of theory (NB-FEP). QM-NBB is then applied to a number of test cases in explicit and implicit solvent with both absolute and relative solvation free energy differences computed. The solutes studied range from frequently used model compounds, such as ethane and methanol, to flexible molecules of up to 30 atoms, e.g., bis-2-chloroethylether and triacetyl glycerol. Further, QM-NBB is compared critically to both the standard FEP based indirect scheme and the newly developed NB-FEP approach. A first large-scale application of the methodology described here to the blind hydration free energy test set of the SAMPL4 competition is reported elsewhere, leading to very good results (König et al., *Predicting hydration free energies with a hybrid QM/MM approach: An evaluation of implicit and explicit solvation models in SAMPL4*, submitted to J. Comput. Aided. Mol. Des.).

2. THEORY

2.1. Standard Methods To Compute Free Energy Differences. Given two states 0 and 1, the free energy difference between them can be computed according to

$$\Delta A(0 \rightarrow 1) = -k_B T \ln \langle \exp[-(U_1 - U_0)/k_B T] \rangle_0 \qquad (2)$$

Here k_B is Boltzmann's constant, T the temperature, and U_0 and U_1 are the potential energies of coordinates evaluated for states 0 and 1, respectively. The angular brackets $\langle \rangle_0$ denote an ensemble average obtained for state 0, i.e., averaging over frames in a trajectory generated in a simulation corresponding to state 0. Equation 2 forms the basis of FEP or thermodynamic perturbation and is commonly attributed to Zwanzig,[92] although the method can be traced back far earlier.[89,93]

Over the past decade, an extension to FEP suggested originally by Bennett[86] and, hence, usually referred to as Bennett's acceptance ratio method (BAR) has become increasingly popular.[82−85,89,94] In contrast to FEP, one needs simulations at both states to compute $\Delta A(0 \rightarrow 1)$.

$$\Delta A(0 \rightarrow 1) = k_B T \left(\ln \frac{\langle f(U_0 - U_1 + C) \rangle_1}{\langle f(U_1 - U_0 - C) \rangle_0} \right) + C \qquad (3)$$

where $f(x)$ denotes the Fermi function $f(x) = (1 + \exp(x/(k_B T)))^{-1}$ and

$$C = k_B T \ln \frac{Q_0 N_1}{Q_1 N_0} \qquad (4)$$

Here, Q_0 and Q_1 are the canonical partition functions of the two states and N_0 and N_1 are the number of data points used to compute the ensemble averages for states 0 and 1, respectively. Equation 3 is iterated until the condition

$$\langle f(U_0 - U_1 + C) \rangle_1 = \langle f(U_1 - U_0 - C) \rangle_0 \qquad (5)$$

is fulfilled. With C determined in this manner, one immediately obtains

$$\Delta A(0 \rightarrow 1) = -k_B T \ln \frac{N_1}{N_0} + C \qquad (6)$$

As already mentioned in the Introduction, BAR has been shown to be much more efficient as compared to FEP for classical FES; i.e., fewer intermediate states are needed to compute a free energy difference of interest.[82−85,89] The need for simulations of both end states, however, has so far prevented the use of BAR to connect MM and QM calculations as MD simulations of sufficient length at the QM end state are too expensive. In classical FES, there is a third, widely used method, thermodynamic integration (TI);[87] however, in connection with QM it is less frequently used and thus not a focus of the current work.[33]

2.2. Unusual Biasing Potentials. Recently, it was shown that results obtained with a relatively cheap (i.e., low computational effort) potential energy function, U^{low}, can be viewed as higher quality results (i.e., more computationally demanding), U^{high}, in the presence of a biasing potential; $V^b = U^{low} - U^{high}$.[91] Classical simulations are the most common basis for sampling conformational space, hence $U^{low} = U^{MM}$, whereas an improved target for FES results would be QM potentials; $U^{high} = U^{QM}$. Thus, in the context of QM FES we consider an MM simulation in the presence of the following biasing potential:

$$V^b = U^{MM} - U^{QM} \qquad (7)$$

Torrie and Valleau showed how to obtain an unbiased ensemble average $\langle X \rangle$ of some property X from simulations of a biased state:[95]

$$\langle X \rangle = \frac{\langle X \exp(\beta V^b) \rangle_b}{\langle \exp(\beta V^b) \rangle_b} \qquad (8)$$

where β has the usual meaning of $1/k_B T$ and we use the notation $\langle \rangle_b$ to indicate that the ensemble averages on the right-hand side of eq 8 are evaluated from simulations of the biased state.

2.3. "Non-Boltzmann" Free Energy Methods. *Non-Boltzmann Bennett.* Applying eq 8 to eq 3 (i.e., BAR) leads to what we call Non-Boltzmann Bennett (NBB).[91] In the context of classical biasing potentials (e.g., accelerated molecular dynamics), this method has also been referred to as weighted BAR.[96] Reference 91 contains several successful examples of free energy simulations based on biased states (i.e., $U = U^{biased}$). In the current work, the computationally cheap MM potential energy function ($U^{low} = U^{MM}$) is used for the exploration of phase space with the QM energy being the ultimate target ($U^{high} = U^{QM}$). Thus, regular classical MD simulations are followed by an analysis of the trajectories at the more exact but computationally demanding QM level of theory. This leads to the equivalent of eq 3 for NBB:

$$\Delta A(0 \to 1) =$$

$$k_B T \ln\left(\frac{\langle f(U_0 - U_1 + C) \exp(\beta V_1^b)\rangle_{1,b} \; \langle \exp(\beta V_0^b)\rangle_{0,b}}{\langle f(U_1 - U_0 - C) \exp(\beta V_0^b)\rangle_{0,b} \; \langle \exp(\beta V_1^b)\rangle_{1,b}} \right) + C \quad (9)$$

The notation follows that of eq 3; however, the additional subscript b indicates that the ensemble averages were obtained in the presence of an unusual biasing potential (eq 7). To use eq 9 it is necessary to evaluate three quantities for each frame of the trajectories: U_0, U_1, and V_0^b for state 0 and U_0, U_1, and V_1^b for state 1. Note that U_0 and U_1 denote the energies *without* the biasing potential, i.e., both the MM and QM energies of interest.

The workflow for NBB is illustrated in Figure 1. In the first step, an MD simulation is conducted for each of the end states,
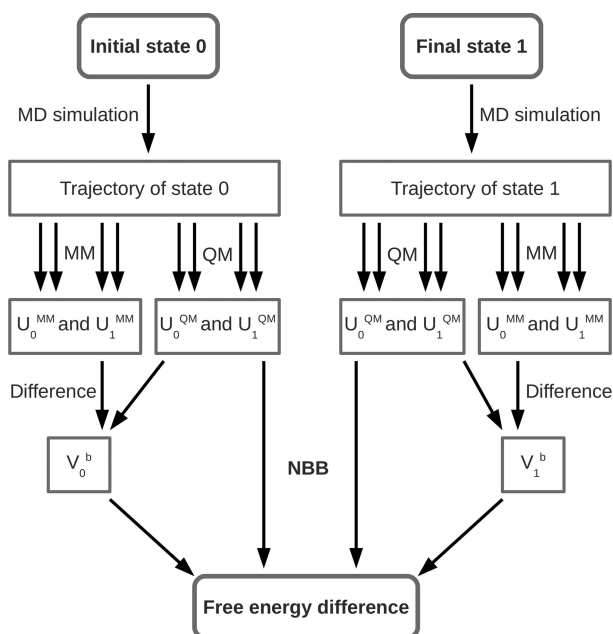
Figure 1. Workflow for using non-Boltzmann Bennett in the hybrid QM/MM free energy simulation approach.

saving coordinates to trajectories at regular intervals. For each frame of the trajectory, state i, the potential energies are evaluated using both MM and QM. The difference between these energies is the biasing potential V_i^b ($i = 0,1$) and is required for NBB. Calculating V^b at every step of the simulation would obviously be cost prohibitive; however, since typically only every hundredth or thousandth MD step is saved, the expensive QM calculations are needed for only a small fraction of the total simulation steps; this greatly reduces the computational cost. In fact, ideally the saving frequency should be long enough to ensure that consecutive data points are statistically independent. In the remainder of this paper, we refer to the use of NBB to connect MM and QM energy surfaces as "QM-NBB" or as *reweighting* from MM to QM.

Non-Boltzmann FEP. In this study we also tested the utility of reweighting from MM to QM based on FEP, which in analogy to NBB we refer to as NB-FEP. Applying eq 8 to eq 2 gives

$$\Delta A(0 \to 1) = -k_B T$$

$$\ln \frac{\langle \exp[-\beta(U_1 - U_0)] \exp(+\beta V_0^b)\rangle_{0,b}}{\langle \exp(+\beta V_0^b)\rangle_{0,b}} \quad (10)$$

As in the case for QM-NBB, U_0 and U_1 are the re-evaluated energies without the biasing potentials; i.e., in the present case the QM energies. Note that the idea of carrying out, e.g., FEP based on simulations in the presence of a biasing potential is hardly new. It was first described by Straatsma and McCammon in 1994[97] and has been gradually rediscovered recently.[91,98] However, in most cases the purpose of the biasing potential was to overcome barriers; the only applications of unusual biasing potentials as employed in this work we are aware of are ref 91 and, to some extent, ref 3.

2.4. Practical Aspects. *Implicit Solvent QM Calculations.* Calculating solvation free energies using an implicit solvent (IS) model is a special case. The free energy difference between the solute in the gas phase and IS can be computed in one step (i.e., no intermediate states), in particular, if BAR is used.[88,99] Thus eq 9 can be used directly. States 0 and 1 represent gas phase and IS, respectively, with separate simulations (e.g., MM and MM/IS) in addition to re-evaluated QM and QM/IS energies required for both. This leads to the generic symbols in eqs 9 and 10 having the following concrete meaning: $U_0 = U^{QM}$, $U_1 = U^{QM/IS}$, and the biasing potentials are $V_0^b = U^{MM} - U^{QM}$, $V_1^b = U^{MM/IS} - U^{QM/IS}$. In all IS calculations presented here, all atoms are treated by either MM or QM (i.e., MM/IS, QM/IS).

Reweighting in Indirect QM FES. In practice, FES usually require intermediate λ states; i.e., one needs to carry out simulations at $\lambda = \lambda_0$, λ_1, ..., λ_{n-1}, λ_n, with $\lambda_0 = 0$ and $\lambda_n = 1$. Since the free energy is a state function, one does not have to reweight every λ-state; it is sufficient to carry out the reweighting only at the end states. This is the basis of the indirect approach to QM FES; Scheme 1. The corresponding *indirect QM-NBB scheme* can be seen in Figure 2. We outline
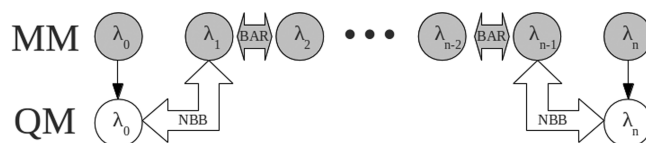
Figure 2. Illustration of the QM-NBB scheme applied to indirect alchemical FES (i.e., reweighting only the end states). Gray nodes represent simulated states, and white nodes are virtual states that are generated through reweighting (thin arrows). Except for the first and the last free energy step, all free energy calculations are performed with regular BAR (eq 3); i.e., without reweighting. The first and the last free energy calculation use NBB to calculate the free energy difference between a virtual QM state and a simulated MM state.

the approach for end state 0. For the analogous steps at state 1 replace λ_0 by λ_{n-1} and λ_1 by λ_n. The MM simulation at, e.g., λ_0 is considered a QM simulation in the presence of the biasing potential $V^b = U^{MM} - U^{QM}$. Together with an MM simulation at λ_1, NBB is used to compute the free energy difference $\Delta A(\lambda_0, \text{QM/MM} \to \lambda_1, \text{MM})$. This should be contrasted with the usual FEP based indirect scheme where $\Delta A(\lambda_0, \text{MM} \to \lambda_1, \text{MM})$ would be computed by some method and combined with $\Delta A(\lambda_0, \text{MM} \to \lambda_0, \text{QM/MM})$.

1409

dx.doi.org/10.1021/ct401118k | *J. Chem. Theory Comput.* 2014, 10, 1406−1419

3. METHODS

3.1. Calculations in Explicit Solvent. All explicit solvent simulations were conducted with CHARMM,[100,101] using the CHARMM22[102] force field. The QM and QM/MM calculations were performed with Q-Chem[103] based on the Q-Chem/CHARMM interface.[104]

Calculation of Alchemical Intermediate States with QM/MM. Many applications of FES involve alchemical mutations of one molecule to another; e.g., to compare binding affinities of two ligands to a particular target or calculate relative solvation free energy differences. Such alchemical mutations are usually realized by mixing the potential energy functions (U) of both end states 0 and 1 as a function of the coupling parameter λ (e.g., $U_\lambda = (1 - \lambda)U_0 + \lambda U_1$) to form artificial intermediate states between the two end states.

In order to evaluate the potential energies U_0 and U_1, the coordinates of the atoms of both end states have to be defined. This can be achieved in two possible ways. The first strategy involves a single topology setup,[105,106] where the bonded and nonbonded parameters of atoms are changed according to λ (e.g., in the mutation of ethane to methanol where the C–C bond length is slowly changed to the C–O bond length). While this approach is viable in MM, it is more problematic for QM or QM/MM approaches. The second approach, dual topology,[105,106] is illustrated for the mutation of ethane to methanol in Figure 3. It involves a hybrid molecule that
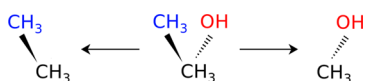
Figure 3. Dual topology setup of a mutation from ethane to methanol. Starting from the hybrid molecule (middle), it is possible to calculate the potential energy of both end states by ignoring all atoms corresponding to the other end state. The system is divided into three groups: The common environment that is present in both end states (black); atoms that only exist in the ethane initial state (blue); and atoms that only exist in the methanol final state (red). The last two groups do not interact with each other.

contains three sets of coordinates: (a) the common environment (atoms that are the same in both end states, e.g., for ethane–methanol the first methyl group shown in black); (b) atoms that exist only in the initial state 0 (e.g., the second methyl group in ethane, shown in blue); and (c) atoms that exist only in the final state 1 (e.g., the hydroxyl group in methanol, shown in red). It is important to ensure that there are no interactions between groups b and c. This approach is easy to implement in QM calculations, as the potential energy evaluations are only performed using coordinates of the pure end states (i.e., to produce the initial state 0, groups a and b are used, while for the final state 1 groups a and c are required).

Ethane–Methanol. Solvation free energy differences between ethane and methanol were calculated using the standard thermodynamic cycle.[107] The dual topology hybrid scheme was implemented using the MSCALE module[108] of CHARMM and follows the recommendations by Boresch and Karplus.[106,109] For the simulations, each energy evaluation was divided into three tasks: calculate energetic contributions of all (a) bond, angle, and Urey–Bradley terms from the full hybrid molecule, $U_{\text{commonbonds}}^{\text{MM}}$ (this was done in the "main" MSCALE process to maintain the connectivity of the hybrid molecule); (b) dihedral angle and nonbonded contributions corresponding to state 0, U_0^{MM} (i.e., all atoms that are not part of ethane or the

common environment were deleted); and (c) dihedral angle and nonbonded contributions corresponding to state 1, U_1^{MM} (i.e., all atoms that are not part of methanol or the common environment were deleted). The λ states were generated by mixing those three energy contributions according to $U_\lambda^{\text{MM}} = U_{\text{commonbonds}}^{\text{MM}} + (1 - \lambda)U_0^{\text{MM}} + \lambda U_1^{\text{MM}}$.

To calculate the biasing potential, V^b, individual potential energies were calculated with Q-Chem and CHARMM based on input files generated by the Q-Chem/CHARMM interface.[104] B3LYP/6-31G* was used to describe the solute in both gas phase and explicit solvent QM/MM calculations (solvent was treated classically with the TIP3P water model). Each frame of the trajectory was calculated as follows: (a) by removing all atoms not corresponding to the initial state 0 (ethane) and calculating the potential energy, U_0^{QM}, and (b) by removing all atoms not corresponding to the final state 1 (methanol) and calculating the potential energy, U_1^{QM}. To calculate the potential energy of λ states, the two terms were mixed according to $U_\lambda^{\text{QM}} = (1 - \lambda)U_0^{\text{QM}} + \lambda U_1^{\text{QM}}$. Of course it is not necessary to compute the terms that are multiplied with zero at the corresponding end state.

Unfortunately, at the time those calculations were conducted, periodic boundary conditions (PBC) and Particle Mesh Ewald (PME) calculations were not supported by Q-Chem. Therefore, the approach to calculate U_λ^{QM} as outlined in the last paragraph could only be used in the gas phase. Instead, the explicit solvent QM/MM calculations in Q-Chem used a single box of water molecules that were centered around the solute for each frame of the trajectory (since no PBCs were used, we refer to this energy as $U_{\text{nopbc}}^{\text{QM/MM}}$). To make the calculation of V^b possible, we also performed MM calculations with CHARMM in exactly the same setup (i.e., without PBC and water molecules centered around the solute, using a cutoff of 999 Å; $U_{\text{nopbc}}^{\text{MM}}$). Thus, $V^b = U_{\text{nopbc}}^{\text{MM}} - U_{\text{nopbc}}^{\text{QM/MM}}$ for the solvent trajectories. To include the effects from periodic boundary conditions in the FES, each U in the QM-NBB calculations consisted of $U^{\text{QM/MM}} = U_{\text{withpbc}}^{\text{MM}} - V^b$, where $U_{\text{withpbc}}^{\text{MM}}$ is the potential energy of the hybrid molecule as used in the simulation (i.e., with PME using CHARMM). This assumes that long-range polarization effects are minimal. To generate potential energies for each λ state, $U^{\text{QM/MM}}$ was evaluated once for the initial state 0 ($U_0^{\text{QM/MM}}$) and once for the final state 1 ($U_1^{\text{QM/MM}}$), leading to $U_\lambda^{\text{QM/MM}} = (1 - \lambda)U_0^{\text{QM/MM}} + \lambda U_1^{\text{QM/MM}}$ for simulations in solution. Correspondingly, the biasing potential for each lambda state V_λ^b is given by $V_\lambda^b = (1 - \lambda)U_{\text{nopbc0}}^{\text{MM}} + \lambda U_{\text{nopbc1}}^{\text{MM}} - (1 - \lambda)U_{\text{nopbc0}}^{\text{QM/MM}} - \lambda U_{\text{nopbc1}}^{\text{QM/MM}}$, where the indices 0 and 1 indicate which end state is used.

Gas phase simulations were conducted with Langevin dynamics, using a friction coefficient of 5 ps^{-1} on all atoms and random forces according to a target temperature of 300 K. In solution, we used 862 water molecules and an octahedral box that was cut from a cube with a side length of 32.168 Å. The temperature was maintained at about 300 K by a Nosé-Hoover thermostat.[110] Lennard-Jones interactions were switched off between 10 and 12 Å, while electrostatic interactions were computed with the PME method.[111] Three different time steps were evaluated: 0.5, 1, and 2 fs. For the last two time steps (1 and 2 fs), we also compared simulations with and without SHAKE on all hydrogen atoms. In the gas phase, the cutoff radius was set to 998 Å.

Free energy differences were calculated based on simulations of 5 ns in gas phase and 1 ns in solution. Trajectories were written every 100 steps in the gas phase and every 20 steps in

solution. For the free energy calculations, 5 λ points were employed in the gas phase (0.00, 0.25, 0.50, 0.75, and 1.00) and 11 in solution (0.0, 0.1, 0.2, 0.3, 0.4, 0.5, 0.6, 0.7, 0.8, 0.9, 1.0). The standard deviations of the free energy results were determined by repeating each simulation four times, starting with different initial random velocities.

Absolute Solvation Free Energies. The classical absolute solvation free energies of ethane and methanol were calculated by turning off all nonbonded interactions of the solute in both gas phase and solution. Since turning off both inter- and intramolecular interactions at the QM level is nontrivial, the indirect FES approach was employed. The alchemical mutation was done in two steps: first, all charges of the solute were set to zero using 6 λ states in gas phase (λ = 0.00, 0.05, 0.15, 0.40, 0.80, and 1.00) and 12 in solution (λ = 0.00, 0.05, 0.10, 0.20, ..., 0.90, and 1.00). QM/MM potential energy calculations were carried out only at λ = 0.00 and λ = 0.05 of the uncharging step. In the second step, all Lennard-Jones interactions of the solute were set to zero, using 7 λ states in gas phase (λ = 0.00, 0.15, 0.35, 0.65, 0.80, 0.90, and 1.00) and 13 in solution (λ = 0.00, 0.05, 0.10, 0.20, ..., 0.90, 0.95, and 1.00). Soft core potentials, as implemented in the PERT module of CHARMM, were employed to avoid the end point problem. Free energy differences were calculated based on simulations of 50 ns in gas phase and 0.5 ns in solution with coordinates saved every 1000 steps and 20 steps, respectively. Simulations were repeated in triplicate with different random seeds to compute standard deviations.

Gas phase simulations were conducted with Langevin dynamics, using a friction coefficient of 5 ps^{-1} on all atoms and random forces according to a target temperature of 300 K. In solution, we used 1492 water molecules and an octahedral box that was cut from a cube with a side length of 38.604 Å. The temperature was maintained at about 300 K by a Nosé-Hoover thermostat. Lennard-Jones interactions were switched off between 10 and 12 Å, while electrostatic interactions were computed with PME. Both molecules were equilibrated for 0.1 ns using constant pressure and, prior to production, each λ point was further equilibrated for 0.1 ns using constant volume.

3.2. Calculations in Implicit Solvent (IS). The reweighting formalism described in Sections 2.2 and 2.4 can be directly applied to solvation free energy calculations employing IS models. Analogous to previous work,[91] we carry out classical gas phase and GBMV[112] IS simulations. Subsequently, the solvation free energy differences were reweighted via NBB to approximate results obtained using DFT (e.g., M06-2X,[113] B3LYP[114,115]) and QM/IS models (e.g., SMD,[116,117] SM8,[103,118] SM12[103,119]). To demonstrate the applicability of QM-NBB, we chose model compounds from two groups. First, a set of amino acid side chain analogues that are neutral at pH = 7 were chosen; these have been established as a gauge for the accuracy and efficiency of free energy simulations.[7,120,121] Second, in a study combining BAR with implicit solvent models Mobley and co-workers pointed out a number of compounds where contributions from solute entropy were expected to be significant;[99] this list included methyl formate, 2-methoxy phenol, bis-2-chloroethylether, 1-octanol, phenyl trifluoroethyl ether, and triacetyl glycerol, which we, therefore, also include in our set. The MM simulations on which the reweighting was based employed the CHARMM36 generalized (CGenFF) and protein force fields.[122,123]
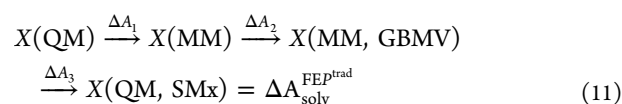
Static QM/IS Calculations. In addition to solvation free energy differences obtained from MD simulations, we also

computed solvation free energy differences based on single coordinate frames. The starting geometry of each solute, taken from the Supporting Information of ref 99, was minimized at the M06-2X/6-31G* level of theory using GAMESS-US[113−115,117] with and without the SMD IS model.[116] ΔA_{solv} is the difference between the minimized energy in the gas phase and in the presence of the SMD model. These data are referred to as "static" SMD results, labeled just "SMD" in Table 5.

Data Generation. CHARMM version c38b1 was used to carry out Langevin dynamics simulations of the model compounds in the gas phase and in GBMV IS. A friction coefficient of 5 ps^{-1} was applied to all atoms. All interactions were included in both gas phase and GBMV simulations; i.e., there was no truncation of nonbonded interactions. The time step in all simulations was 0.5 fs, and the molecules were fully flexible; no bond-length constraints were used. For each solute, at least 5000 coordinate sets were saved in the gas phase and in solution; see the third column in Table 5. The time interval for saving consecutive coordinates Δt is specified in the fourth column of Table 5. The total simulation length in gas phase and implicit solvent, respectively, for a particular compound was, therefore, the number of coordinate sets times Δt; it ranged from 100 ns (e.g., propane) to 500 ns (bis-2-chloroethylether, triacetylglycerol).

Analysis. For each of the coordinates saved, both classical and QM energies were recomputed (gas phase and IS - GBMV, SMx (x = D, 8, 12)). Benchmark results for SMx models were examined and the M06-2X/6-31G* level of theory was determined appropriate for SMD and SM8 IS models while B3LYP/6-31G* showed good performance for the SM12 model. All SMD calculations were carried out with GAMESS-US[117] while SM8/SM12 results were generated with Q-Chem.[103] Initially, classical simulation data was used to estimate the solvation free energy differences (i.e., gas phase → GBMV); referred to as "GBMV". Second, NBB was applied to the forward and backward energy differences obtained from QM/IS calculations, treating the differences between MM and QM energies for the respective reference state as the "biasing" potential. These results are referred to as "SMD,NBB", "SM8,NBB", etc.

In addition to using QM-NBB, the raw data were also evaluated by FEP and NB-FEP (SMD only). For these, the standard thermodynamic cycle of indirect QM FES (Scheme 1) was used; applied to the calculation of ΔA_{solv} for a solute X using an IS model, the scheme shown in Figure 2 simplifies to

$$X(\text{QM}) \xrightarrow{\Delta A_1} X(\text{MM}) \xrightarrow{\Delta A_2} X(\text{MM, GBMV})$$
$$\xrightarrow{\Delta A_3} X(\text{QM, SMx}) = \Delta A_{solv}^{FEP^{trad}} \qquad (11)$$

Here, ΔA_2 is the classical GBMV result. ΔA_1 and ΔA_3 were computed by FEP, perturbing from the end points of the MM FES to the corresponding QM target states. We refer to results obtained in this manner as "traditional" FEP (FEP^{trad}). Next, based on classical gas phase and GBMV simulations, NB-FEP (eq 10) was applied to estimate both the "forward" (FW; QM → QM/IS) and "backward" (BW; QM/IS → QM) directions, respectively. Similar to QM-NBB, the difference between MM and QM energies for the respective reference state was considered the biasing potential, V^b.

Estimating Error. All free energy differences, regardless of method, reported in Table 5 are the values obtained from the full data set. The standard deviations reported were calculated as follows. Free energy differences for blocks of 1000

coordinate frames were calculated, and the standard deviation of these block averages is reported. Given that the coordinate frames should already be almost statistically independent ($\Delta t \geq$ 20 fs), this is likely to overestimate the statistical error; yet the number gives some feeling for the variability of the data. We also always compared ΔA_{solv} computed from the full data and the mean value of the block averages. If the calculations are converged, the two values should be identical. Any discrepancies between these two numbers indicate that the results are not (fully) converged.

4. RESULTS AND DISCUSSION

4.1. Calculations in Explicit Solvent. *Relative Solvation Free Energy Difference between Ethane and Methanol.* Many applications of FES involve alchemical mutations of one molecule to another to predict relative free energies. Further, many systems of interest are poorly described by current classical force fields. Therefore, the capability to efficiently and accurately conduct QM alchemical FES is of critical importance. Here, we evaluate the performance of the proposed QM-NBB approach for a simple mutation of ethane to methanol in water. Calculation of the corresponding solvation free energy difference ($\Delta\Delta A_{solv}$) has become somewhat of a benchmark for FES.[124] A variety of MM force fields yield highly accurate results within very short simulation lengths. Therefore, this system is a useful test for computationally expensive QM free energy methods, as different approaches can be evaluated within reasonable time.

In Table 1 we compare the results of FES based on MM with BAR (MM-BAR, left) and the QM-NBB approach (QM-NBB,

Table 1. Free Energy Differences between Ethane and Methanol (kcal/mol)

	MM-BAR	QM-NBB	Exp.[a]
ΔA_{gas}	+6.02 ± 0.01	−22517.95 ± 0.01	-
ΔA_{H_2O}	−0.86 ± 0.02	−22524.91 ± 0.04	-
$\Delta\Delta A_{solv}$ [b]	−6.89 ± 0.02	−6.96 ± 0.01	−6.93

[a]Experiment: ref 125. [b]Relative solvation free energy difference: $\Delta\Delta A_{solv} = \Delta A_{H_2O} - \Delta A_{gas}$.

middle). The first row gives the free energy difference between ethane and methanol in the gas phase (ΔA_{gas}), while the second row represents the corresponding free energy change in aqueous solution (ΔA_{H_2O}). Subtracting ΔA_{gas} from ΔA_{H_2O} leads to the solvation free energy difference, $\Delta\Delta A_{solv}$, which is shown in the last row together with the experimental reference result (Exp., rightmost column).[125] Both MM-BAR and QM-NBB are in excellent agreement with experiment (deviations of 0.04 and 0.02 kcal/mol). While this small difference in accuracy between MM-BAR and QM-NBB is probably fortuitous, it is still an indicator that QM-NBB FES can lead to improved accuracy even in cases where the MM parameters are well developed.

Obviously, the QM data for ΔA_{gas} and ΔA_{H_2O} are orders of magnitude larger than the corresponding MM-BAR results. This reflects the differences in internal energies between ethane and methanol (i.e., the energetic costs of creating the atoms in the respective method). The major contribution to the internal energy in QM methods arises from the interactions between core electrons and the nuclei. In particular for systems consisting of different numbers of atoms, this results in large

differences in internal energies. However, such electron−nuclei interactions are not present in MM methods, since they do not contribute to the chemical bond. In other words, the apparent discrepancies between MM and QM single free energy differences ΔA_{gas} and ΔA_{H_2O} reflect the different reference states of the methods. It should be pointed out that the single free energy differences for MM would also be very different if another force field had been used (cf., Figure 1 of ref 88). Strictly speaking, only the difference between ΔA_{gas} from ΔA_{H_2O}, which leads to $\Delta\Delta A_{solv}$ in the last row, is of relevance, as the effect of the arbitrary reference state cancels out. The only practical ramification of the large values in QM is that the computer codes for NBB or BAR have to be stable numerically. This is easily accomplished by factoring out large offsets and/or using a suitable starting value for C in eqs 3 and 9.

In Table 2, we compare experimental solvation free energies ($\Delta\Delta A_{solv}^{Exp}$, first column) with QM-NBB results ($\Delta\Delta A_{solv}^{QM-NBB}$,

Table 2. Comparison of Relative Solvation Free Energies for Ethane and Methanol from Several Approaches Based on the Same Set of QM Potential Energy Data[a]

	$\Delta\Delta A_{solv}^{Exp}$ [b]	$\Delta\Delta A_{solv}^{QM-NBB}$ [c]	$\Delta\Delta A_{solv}^{QM-BAR}$ [d]	$\Delta\Delta A_{solv}^{FEP^{trad}}$ [e]
ethane−methanol	−6.93	−6.96 ± 0.04	−6.09 ± 0.02	−7.14 ± 0.09

[a]All energies are reported in kcal/mol. [b]Experiment: ref 125. [c]QM-NBB. [d]QM-BAR (i.e., no reweighting is employed for QM data). [e]Zwanzig's equation (i.e., the traditional FEP approach).

second column) and alternative free energy methods to analyze the same set of QM potential energy data (columns three and four). All computational results presented in this section are based on the same set of trajectories. Thus, any errors resulting from sampling should be consistent and provide a fair test environment for a relative evaluation of accuracy and precision.

One conceivable alternative to QM-NBB consists of using BAR with the QM potential energy data (which does not involve reweighting). This approach assumes that all frames in the MM trajectory are generated with the correct Boltzmann probability in regard to the QM energy surface. The results for $\Delta\Delta A_{solv}^{QM-BAR}$ are shown in the third column of Table 2. As can be seen, the omission of any kind of reweighting step in the workflow leads to errors of about 0.8 kcal/mol. This large deviation illustrates that a correction for the change of probabilities from the MM to the QM energy surface is absolutely necessary. Interestingly, the standard deviation of $\Delta\Delta A_{solv}^{QM-BAR}$ is the same as for pure MM (c.f. last row of MM-BAR in Table 1). This indicates that QM-NBB suffers from some loss of precision (σ 0.04 vs 0.02) and that it is not a result of using QM energies instead of MM but rather an effect of changing the weights of the frames with NBB.

The second alternative consists of using Zwanzig's exponential FEP formula[92] instead of NBB; i.e., the traditional approach according to Scheme 1. In contrast to BAR or NBB that employ two trajectories per FES, FEP uses only a single trajectory, which lowers computational costs. The corresponding results are shown in the rightmost column of Table 2 ($\Delta\Delta A_{solv}^{FEP^{trad}}$). As can be seen, the use of FEP leads to a deviation of 0.21 kcal/mol from experiment. While this deviation might be considered acceptable for standard applications of FES, it is an order of magnitude higher than the QM-NBB deviation (0.03 kcal/mol). In addition, the standard deviation (0.09 kcal/

Table 3. QM-NBB Solvation Free Energy Results from Simulations with Different Time Steps (δt) and with and without SHAKE[a]

	$\Delta\Delta A_{\text{solv}}^{0.5\text{fs}}$[b]	$\Delta\Delta A_{\text{solv}}^{1.0\text{fs}}$[c]	$\Delta\Delta A_{\text{solv}}^{1.0\text{fs/SHAKE}}$[d]	$\Delta\Delta A_{\text{solv}}^{2.0\text{fs/SHAKE}}$[e]	$\Delta\Delta A_{\text{solv}}^{\text{Exp}}$[f]
ethane−methanol	−6.96 ± 0.06	−6.96 ± 0.04	−6.65 ± 0.02	−6.45 ± 0.02	−6.93

[a]All energies are reported in kcal/mol. [b]QM-NBB, δt = 0.5 fs, No SHAKE. [c]QM-NBB, δt = 1.0 fs, No SHAKE. [d]QM-NBB, δt = 1.0 fs, SHAKE. [e]QM-NBB, δt = 2.0 fs, SHAKE. [f]Experiment: ref 125.

mol) is more than twice that of QM-NBB (0.04 kcal/mol). The poor performance of FEP here agrees with recent observations for MM FES,[82−84] where FEP was considerably less accurate and precise than all other free energy methods.

Influence of Time Step and SHAKE. One main difference between MM and QM/MM is the treatment of chemical bonds. Most MM simulations replace the Morse potential of bonds by a harmonic potential. Far from the equilibrium bond length, the errors incurred by this approximation can be considerable. One common way to avoid this problem consists of using SHAKE to keep bond lengths fixed at their equilibrium distances, thus avoiding errors from the harmonic approximation. As a side effect, SHAKE also allows the use of larger time steps in molecular dynamics simulations, leading to improved sampling and thus higher efficiency. One potential drawback to this approach, however, comes from the neglect of anharmonicity, i.e., nonharmonic behavior upon bond stretching.

Table 3 reports data used to analyze the effects of SHAKE and simulation time step on the accuracy of QM-NBB FES. In particular, we compare the performance of simulations that use 0.5 and 1 fs time steps without SHAKE ($\Delta\Delta A_{\text{solv}}^{0.5\text{fs}}$ and $\Delta\Delta A_{\text{solv}}^{1.0\text{fs}}$) as well as simulations with 1 and 2 fs time steps with SHAKE ($\Delta\Delta A_{\text{solv}}^{1.0\text{fs/SHAKE}}$ and $\Delta\Delta A_{\text{solv}}^{2.0\text{fs/SHAKE}}$). Notably, 2 fs time steps are only possible when using SHAKE, so the two sets of 1 fs time step simulations serve as a control to possible errors resulting from SHAKE.

As illustrated in Table 2, using time steps of 0.5 and 1 fs without SHAKE (first two columns) has negligible effect on accuracy. Notably, there is a small difference in terms of precision (standard deviation of 0.06 vs 0.04 kcal/mol), which likely can be attributed to sampling since simulation time doubles when going from 0.5 fs →1.0 fs. Therefore, a 1 fs time step is recommended in the underlying simulations used in QM-NBB FES; however, when high frequency bond stretching is expected to significantly contribute to free energy differences, a smaller time step may be required.

To determine the effect of SHAKE, two 1 fs time step simulations are employed (with and without SHAKE, second and third column, respectively). While the deviation from experimental results is small for the FES without SHAKE (0.03 kcal/mol), the error becomes significantly higher when using SHAKE (0.28 kcal/mol). Notably, a similar error is found for MM-BAR FES of the same trajectories, where the computed solvation free energy difference is −6.73 kcal/mol (error of 0.20 kcal/mol). However, the accuracy deteriorates further when a time step of 2 fs with SHAKE is used, yielding an error of almost 0.5 kcal/mol. This is significantly higher than the error of the underlying MM-BAR FES, which yields a result of −6.76 kcal/mol (error of 0.17 kcal/mol). This suggests that the difference in fixed versus flexible X−H bond treatment (X = N, C, O) can have a significant effect on the free energy when QM-based FES are employed.

To gain additional insight into errors associated with SHAKE, both standard harmonic and anharmonic gas phase

QM calculations were carried out on ethane and methanol using the transition-optimized shifted Hermite (TOSH) method.[126] From Table 2, the energetic penalty of using SHAKE on the 1 fs simulations is 0.31 kcal/mol. This appears to be a result of limiting high frequency bond stretching in two systems where the effects do not cancel; i.e., a larger effect in methanol due to its O−H bond. Calculations at the B3LYP/6-31G* level of theory seemingly confirm this. Examining ΔS_{total} (= $S_{\text{total}}^{\text{Anharm}} - S_{\text{total}}^{\text{Harm}}$) reveals that 0.21 kcal/mol of entropy is gained for methanol upon accounting for anharmonicity whereas 0.09 kcal/mol is lost in ethane. This yields a total effect of 0.30 kcal/mol, in near perfect agreement with QM-NBB results (vide supra). This should serve as another point of caution for approaches that connect MM ↔ QM using either fixed or restrained QM regions.[77−79]

Absolute Solvation Free Energies of Ethane and Methanol. The calculation of absolute solvation free energies involves the gradual deactivation of solute−solvent interactions until the solute is in a noninteracting ideal gas state. This process requires scaling all solute−solvent interactions and naturally leads to the application of the indirect FES scheme. Table 4 reports the performance of both MM and QM/MM

Table 4. Absolute solvation free energies for ethane and methanol[a]

	$\Delta A_{\text{solv}}^{\text{MM−BAR}}$[b]	$\Delta A_{\text{solv}}^{\text{QM-NBB}}$[c]	$\Delta A_{\text{solv}}^{\text{Exp}}$[d]
ethane	2.29 ± 0.10	2.03 ± 0.10	1.83
methanol	−4.68 ± 0.03	−4.82 ± 0.04	−5.10
RMSD[e]	0.42	0.22	

[a]All energies are reported in kcal/mol. [b]MM-BAR FES. [c]QM-NBB, indirect FES approach. [d]Experiment: ref 125. [e]RMSD from experimental results.

based results for ethane and methanol. The MM results are shown in the first column, while the QM-NBB results are shown in the second. Again, the difference between MM and QM/MM is statistically significant. Both methods show good agreement with experiment; root-mean-square deviations, RMSD, are about 0.4 and 0.2 kcal/mol, respectively (see last row of Table 4). Of note, RMSD results indicate that the previously observed excellent experimental agreement ($\Delta\Delta A_{\text{solv}}$, Table 2) was fortuitous and likely a result of cancellation of errors. Nevertheless, it is also clearly demonstrated that significant error reduction can be realized when applying QM-NBB FES.

4.2. Calculations in Implicit Solvent. In Table 5 we report ΔA_{solv} for 21 compounds, ranging in size from 5 to 29 atoms; see the second column in the table. Aside from the experimental values, taken from the Supporting Information of ref 99, we report computed free energy differences obtained by BAR based on the MM gas phase and GBMV raw data, by DFT/SMD based on a single coordinate set, and by QM-NBB based on the reweighting to DFT/SMD, as well as DFT/SMD results obtained by FEP and NB-FEP (cf. Methods). Results

Table 5. Simulation Details for and Results of Absolute Solvation Free Energy Difference Calculations Based on Implicit Solvent Models[a]

compound	atoms[b]	no. pts[c]	Δt, ps[d]	exp.[e]	GBMV[f]	SMD[g]	SMD,NBB[h]	SMD,FEP$^{\text{trad}}$[i]	NB-FEP,fw[j]	NB-FEP,bw[k]
methane	5/1	5000	20	1.99	1.35	2.23	2.17 ± 0.03	2.16 ± 0.07	2.16	−2.17
ethane	8/2	15 000	20	1.83	1.33	1.83	1.76 ± 0.03	1.74 ± 0.11	1.77	−1.75
propane	11/3	5000	20	1.96	1.37	1.91	1.88 ± 0.01	1.61 ± 0.27	1.88	−1.88
i-butane	14/4	5000	20	2.32	1.47	2.22	2.21 ± 0.01	2.27 ± 0.36	2.20	−2.21
n-butane	14/4	10 000	40	2.07	1.52	2.11	2.09 ± 0.03	1.87 ± 0.28	2.05	−2.12
methanol	6/2	15 000	20	−5.10	−5.27	−3.88	-4.00 ± 0.09	-3.98 ± 0.31	−4.06	3.92
ethanol	9/3	5000	20	−5.00	−4.96	−3.60	-3.85 ± 0.06	-5.20 ± 0.90	−3.71	3.97
methanethiol	6/2	5000	20	−1.24	−0.29	−0.88	-0.78 ± 0.08	-1.16 ± 0.26	−0.76	0.79
ethyl-methylsulfide	12/4	5000	20	−1.50	1.09	−0.33	-0.30 ± 0.09	0.08 ± 0.26	−0.36	0.26
methylformate	8/4	12 500	40	−2.78	−6.39	−1.62	-1.67 ± 0.07	-1.78 ± 1.59	−1.63	1.67
2-methoxyphenol	17/9	5000	50	−5.57	−4.42	−1.06	-3.33 ± 0.13	-2.67 ± 0.33	−3.39	3.05
bis-2-chloroethylether	15/7	10 000	50	−4.23	−3.04	−5.24	-4.02 ± 0.49	-2.34 ± 1.27	−4.46	4.07
1-octanol	27/9	5000	60	−4.09	−3.62	−1.88	-2.42 ± 0.28	-2.50 ± 0.65	−2.46	2.35
phenyl-trifluoroethyl-ether	19/12	5000	60	−1.29	−2.88	−1.60	-0.57 ± 0.13	-3.21 ± 2.33	−0.67	0.56
triacetylglycerol	29/15	5000	100	−8.84	−14.55	−7.21	-6.37 ± 0.36	-4.02 ± 2.70	−6.09	6.54
acetamide	9/4	5000	20	−9.68	−8.95	−7.96	-7.98 ± 0.28	-9.02 ± 0.58	−7.18	8.57
propionamide	12/5	5000	20	−9.38	−8.56	−7.43	-7.15 ± 0.29	-7.65 ± 0.55	−7.32	7.05
4-methylimidazole	12/6	5000	20	−10.27	−11.27	−7.81	-8.05 ± 0.18	-8.81 ± 0.41	−8.01	8.08
toluene	15/7	5000	20	−0.89	0.11	−0.14	-0.12 ± 0.04	0.59 ± 0.90	−0.15	0.10
p-cresol	16/8	5000	20	−6.13	−4.46	−3.41	-3.69 ± 0.03	-4.30 ± 0.87	−3.75	3.58
3-methylindole	19/9	5000	20	−5.88	−5.50	−3.64	-3.35 ± 0.11	-3.50 ± 0.50	−3.45	3.25

[a]All solvation free energies are in kcal/mol. [b]Number of atoms/number of non-hydrogen atoms. [c]Total number of conformations used to compute ΔA_{solv} by the various methods. [d]Time interval for saving conformations. [e]Experimental ΔA_{solv} taken from the Supporting Information ref 99. [f]ΔA_{solv} based on the classical GBMV implicit solvent model calculated with BAR. [g]"Static" ΔA_{solv} calculated with the quantum chemical SMD implicit solvent model based on a single conformation. [h]ΔA_{solv} based on the quantum chemical SMD implicit solvent model calculated with NBB. [i]$\Delta A_{\text{solv}}^{\text{FEP}^{\text{trad}}}$ based on the quantum chemical SMD implicit solvent model calculated from the classical GBMV result plus corrections between classical and quantum chemical description computed with FEP; cf. eq 11 and Scheme 1. [j]ΔA_{solv} based on the quantum chemical SMD implicit solvent model calculated with NB-FEP in the forward direction [k]ΔA_{solv} based on the quantum chemical SMD implicit solvent model calculated with NB-FEP in the backward direction.

Table 6. Simulation Results of Absolute Solvation Free Energy Difference Calculations Based on QM Implicit Solvent Models SMD, SM8, and SM12[a]

	exp.	GBMV	SMD,NBB	SM8,NBB	SM12,NBB
methane	1.99	1.35	2.17	1.72 ± 0.01	1.33 ± 0.01
ethane	1.83	1.33	1.76	1.12 ± 0.01	0.82 ± 0.01
propane	1.96	1.37	1.88	1.12 ± 0.01	0.85 ± 0.01
i-butane	2.32	1.47	2.21	1.42 ± 0.01	1.12 ± 0.01
n-butane	2.07	1.52	2.09	1.21 ± 0.01	0.97 ± 0.01
methanol	−5.10	−5.27	−4.00	-4.88 ± 0.01	-5.02 ± 0.02
ethanol	−5.00	−4.96	−3.85	-4.71 ± 0.07	-4.91 ± 0.08
methanethiol	−1.24	−0.29	−0.78	-0.50 ± 0.01	-1.11 ± 0.01
ethyl-methylsulfide	−1.50	1.09	−0.30	-0.42 ± 0.05	-0.70 ± 0.03
methyl formate	−2.78	−6.39	−1.67	-2.56 ± 0.04	-3.12 ± 0.03
2-methoxy phenol	−5.57	−4.42	−3.33	-5.40 ± 0.09	-6.14 ± 0.04
bis-2-chloroethylether	−4.23	−3.04	−4.02	-3.66 ± 0.14	-4.16 ± 0.11
1-octanol	−4.09	−3.62	−2.42	-3.45 ± 0.05	-3.49 ± 0.04
phenyl-trifluoroethyl-ether	−1.29	−2.88	−0.57	-1.89 ± 0.06	-2.26 ± 0.09
triacetyl glycerol	−8.84	−14.55	−6.37	-9.03 ± 0.19	-9.71 ± 0.14
acetamide	−9.68	−8.95	−7.98	-10.93 ± 0.17	-10.89 ± 0.04
propionamide	−9.38	−8.56	−7.15	-10.57 ± 0.30	-10.58 ± 0.10
4-methylimidazole	−10.27	−11.27	−8.05	-9.18 ± 0.19	-8.84 ± 0.08
toluene	−0.89	0.11	−0.12	-0.95 ± 0.01	-1.17 ± 0.01
p-cresol	−6.13	−4.46	−3.69	-5.35 ± 0.04	-5.58 ± 0.02
3-methylindole	−5.88	−5.50	−3.35	-4.66 ± 0.05	-4.79 ± 0.01
RMSD[b]		1.79	1.47	0.76	0.85

[a]All solvation free energies are in kcal/mol. [b]RMSD of the solvation free energy compared to the experimental result.

obtained by reweighting to DFT/SM8 and DFT/SM12 are shown in Table 6; cf. below.

The classical force field combined with the GBMV implicit solvation model (column "GBMV" in Table 5) does reasonably well for most compounds; however, there are some severe errors, such as for ethyl-methylsulfide, methyl formate, and triacetyl glycerol. The statistical error of all results is extremely low (<0.1 kcal/mol in all cases, data not shown); thus, the results reflect the strengths and weaknesses of the classical force field and solvation model.

Overall, the results obtained with DFT and the SMD solvation model, based both on single configurations (column "SMD") and QM-NBB (column "SMD,NBB"), are in better agreement with experiment. There are fewer huge outliers compared to MM/GBMV; yet, the results for alcohols are somewhat disappointing and unexpected. Much better agreement with experiment is obtained with the SM8 and SM12 solvation models, cf. Table 6. The last line in this table lists the RMSDs of the computed ΔA_{solv} results relative to experiment. While SMD (1.47 kcal/mol) is an improvement over GBMV (1.79 kcal/mol), it compares poorly to the values of 0.76 and 0.85 kcal/mol for SM8 and SM12. Interestingly, the newer SM12 model fares slightly worse than its predecessor SM8 for this particular set of 21 compounds; however, this could be a consequence of the functional and grid employed (B3LYP (SG-1) vs M06-2X (99,590), respectively).

The focus of this study is not a critical evaluation of implicit solvation models. Instead, it is more interesting to note that introducing flexibility has a large influence on results in some cases, e.g., bis-2-chloroethylether or phenyl-trifluoroethyl-ether, where static and MD based results differ by over 1 kcal/mol. Overall, the QM-NBB results are in slightly better agreement with experiment (i.e., SMD vs SMD,NBB results in Table 5). The standard deviation is quite low in most cases; the largest variation of results was observed for bis-2-chloroethylether. However, the difference between the free energy difference obtained for the full data set and the average of the individual blocks (cf. Methods) is less than 0.1 kcal/mol for all solutes, i.e., well below the statistical error estimated based on the standard deviation of the block results. This indicates that the results are well converged; e.g., for bis-2-chloroethylether, although the standard deviation is ±0.49 kcal/mol, the discrepancy is only 0.02 kcal/mol (data not shown).

While our QM-NBB approach performs well and leads to converged results in all cases, the standard indirect approach (FEP^{trad}) based on FEP from MM → QM (eq 11) is problematic. It does work for small molecules, e.g., methane or ethane. In those cases, the FEP^{trad} result (see column "SMD,FEP^{trad}") agrees with the QM-NBB result, the standard deviation is low, and the free energy difference obtained from all data agrees with the average of the block results (data not shown). However, already for, e.g., propane with FEP^{trad}, the quality of the result is noticeably poorer than QM-NBB; differing by more than 0.2 kcal/mol with considerably higher standard deviation (±0.27 kcal/mol for FEP^{trad} vs ±0.01 for QM-NBB). For larger molecules, e.g., toluene, the FEP^{trad} results are unusable. The standard deviation is now almost 1 kcal/mol, while the free energy difference obtained from all data (0.59 kcal/mol) is quite different from the average of the block results (0.1 kcal/mol, data not shown); both values differ noticeably from the QM-NBB result (−0.12 kcal/mol).

By contrast, NB-FEP performs surprising well. In most cases, the NB-FEP results agree within error bars with QM-NBB; the

QM-NBB result is usually close to the average value of the forward and backward NB-FEP result. However, for larger molecules the hysteresis between forward and backward results increases. The outlier is acetamide, where the hysteresis is over 1 kcal/mol; this is the only case where the forward and backward result cannot be reconciled based on the statistical error estimate. Given that the computational effort of doing NB-FEP in both forward and backward direction is comparable to that of QM-NBB, the latter is clearly advantageous.

Several of the compounds studied can adopt multiple conformations that require sufficient sampling, the simplest example being butane. In ref 94 the authors observed that the central dihedral angle of butane was poorly sampled even in simulations of 1 ns length, cf. their Figure 7.

Figure 4 shows the degree of sampling of the central dihedral angle of butane in the data used for the reweighting. The red
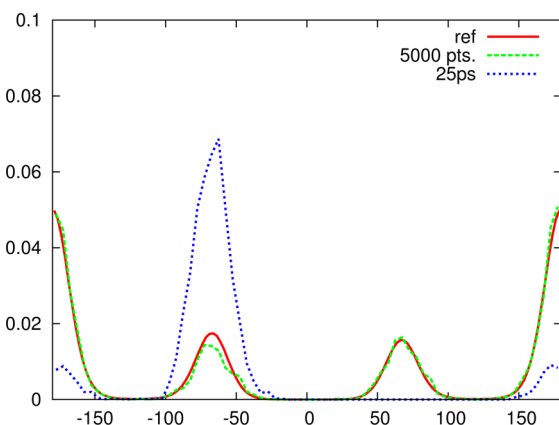
Figure 4. Sampling of butane's conformational space. The x-axis is butane's central dihedral angle while the y-axis is probability.

line is a reference histogram obtained from a separate 500 ns simulation, whereas the green curve displays the histogram obtained from the 10 000 data points (gas phase) used in the free energy simulations. The two curves are practically identical. The data underlying our FES (green curve) should be contrasted to the amount of sampling achieved in a simulation of just 50 000 MD steps, saving every 10th step (blue line). One gauche minimum is not sampled at all, and the other gauche minimum and the trans minimum have wrong weights. Of course, 50 000 MD steps may seem ridiculously short, but a brute force simulation with a QM potential as used in this work for reweighting (DFT - M06-2X, SMD, or SM8 IS model) would already be a significant computational undertaking. Performing a 1 ns simulation, the simulation length used in the study by Shirts et al.[94] would be prohibitively expensive even today. The present implicit solvent work relied on regular long MD simulations for sufficient sampling, as the MM simulations are cheap compared to re-evaluation at the QM level. However, the approach would work equally well (or even better) if enhanced sampling techniques would have been used to generate conformations for reweighting; evaluation of this is already underway.

5. CONCLUSIONS

Two new approaches (QM-NBB and NB-FEP) are presented for effectively connecting MM simulations with QM calculations to determine free energy differences. Both methods are based on the use of "unusual" biasing potentials to obtain more

accurate results; i.e., simulations carried out at low levels of theory (MM) in conjunction with high level (QM) potential energy evaluations. QM-NBB is initially applied to calculate both absolute and relative solvation free energy differences of ethane and methanol in explicit solvent. Our results demonstrate that the reweighting step is necessary. Just inserting the QM energies into regular BAR ("QM-BAR" in Table 2) leads to a clearly erroneous result. This can be explained by the differences in the underlying MM and QM potential energy surfaces; i.e., the ensemble of "important" states on the two surfaces are significantly different. The effect of those differences can be aggravated by constraining degrees of freedom with SHAKE (Table 3). In this case, the results became incorrect because the MM and QM description of the system did not match. Quite generally, the potential energy surface at which sampling is carried out has to be, to some degree, representative of the QM surface, with mismatches being caused by a variety of energetic components; e.g., electrostatics, harmonic approximates, and more. While two-sided methods such as BAR/NBB are much more efficient than, e.g., FEP, some minimal amount of overlap is required. However, if sampling is adequate, QM-NBB leads to a more accurate and precise result than the traditional indirect scheme coupled with FEP ($\Delta\Delta A_{solv}^{FEP^{trad}}$ in Table 2).

The computation of solvation free energies for a diverse series of 21 compounds further validates the usefulness of these new approaches. The employed compounds range from small molecules to fairly large, flexible solutes, such as triacetyl glycerol, and, therefore, can be considered representative of practical FES applications. Triacetyl glycerol is an example of a compound where force fields result in poor solvation free energies (cf. "GBMV" in Table 5 and Supporting Information of ref 99). The traditional FEP approach for QM/MM FES also leads to inaccurate results, as it becomes numerically unstable or completely unusable for systems much larger than 10 atoms. NB-FEP greatly improved performance compared to standard FEP; however, numerical inconsistencies were still observed. Thus, QM-NBB is established as the preferred method to connect MM to QM (or QM/MM) levels of theory. This is clearly reflected by comparisons to experiment. The combination of a classical force field with BAR and the GBMV implicit solvent model leads to a RMSD of 1.79 kcal/mol while the use of QM-NBB with SM8 reduces this RMSD to 0.76 kcal/mol. To put those numbers into perspective, the best results of the SAMPL0 to SAMPL2 prediction competitions exhibited RMSDs between 1.3 and 3.6 kcal/mol.[21,24,127,128]

While the quality of traditional MM FES strongly depends on the selected parameters (in particular charges),[129] conventional QM solvation free energy evaluations based on a single conformation can suffer from not accounting for solute entropy. QM-NBB overcomes these weaknesses by combining the strengths of both approaches: efficient sampling from MM and accurate intra- and intermolecular interactions from QM. Thus, QM-NBB with the right choice of QM level of theory holds significant promise as an "affordable" method for calculating highly accurate free energies, e.g., on par with or better than standard methods currently being employed.

■ AUTHOR INFORMATION

Corresponding Authors
*(S.B.) E-mail: stefan@mdy.univie.ac.at.
*(H.L.W.) E-mail: hlw@usf.edu.

■ REFERENCES

(1) Oostenbrink, C.; van Gunsteren, W. Free energies of ligand binding for structurally diverse compounds. *Proc. Natl. Acad. Sci. U.S.A.* **2005**, *102*, 6750−6754.

(2) Mobley, D. L.; Graves, A. P.; Chodera, J. D.; McReynolds, A. C.; Shoichet, B. K.; Dill, K. A. Predicting absolute ligand binding free energies to a simple model site. *J. Mol. Biol.* **2007**, *371*, 1118−1134.

(3) Shirts, M. R.; Mobley, D. L.; Chodera, J. D.; Pande, V. S. Accurate and efficient corrections for missing dispersion interactions in molecular simulations. *J. Phys. Chem. B* **2007**, *111*, 13052−13063.

(4) de Ruiter, A.; Oostenbrink, C. Efficient and Accurate Free Energy Calculations on Trypsin Inhibitors. *J. Chem. Theory Comput.* **2012**, *8*, 3686−3695.

(5) de Ruiter, A.; Boresch, S.; Oostenbrink, C. Comparison of thermodynamic integration and Bennett's acceptance ratio for calculating relative protein-ligand binding free energies. *J. Comput. Chem.* **2013**, *34*, 1024−1034.

(6) Deng, Y.; Roux, B. Computations of standard binding free energies with molecular dynamics simulations. *J. Phys. Chem. B* **2009**, *113*, 2234−2246.

(7) Shirts, M. R.; Pitera, J. W.; Swope, W. C.; Pande, V. S. Extremely precise free energy calculations of amino acid side chain analogs: Comparison of common molecular mechanics force fields for proteins. *J. Chem. Phys.* **2003**, *119*, 5740−5761.

(8) Pitera, J. W.; van Gunsteren, W. F. One-Step Perturbation Methods for Solvation Free Energies of Polar Solutes. *J. Phys. Chem. B* **2001**, *105*, 11264−11274.

(9) Seeliger, D.; de Groot, B. Protein Thermostability Calculations Using Alchemical Free Energy Simulations. *Biophys. J.* **2010**, *98*, 2309−2316.

(10) König, G.; Bruckner, S.; Boresch, S. Absolute Hydration Free Energies of Blocked Amino Acids: Implications for Protein Solvation and Stability. *Biophys. J.* **2013**, *104*, 453−462.

(11) Gao, J.; Li, N.; Freindorf, M. Hybrid QM/MM Simulations Yield the Ground and Excited State pK_a Difference: Phenol in Aqueous Solution. *J. Am. Chem. Soc.* **1996**, *118*, 4912−4913.

(12) Li, G.; Cui, Q. pKa Calculations with QM/MM Free Energy Perturbations. *J. Phys. Chem. B* **2003**, *107*, 14521−14528.

(13) Riccardi, D.; Schaefer, P.; Cui, Q. pKa calculations in solution and proteins with QM/MM free energy perturbation simulations: a quantitative test of QM/MM protocols. *J. Phys. Chem. B* **2005**, *109*, 17715−17733.

(14) Riccardi, D.; Cui, Q. pKa analysis for the zinc-bound water in human carbonic anhydrase II: Benchmark for "multiscale" QM/MM simulations and mechanistic implications. *J. Phys. Chem. A* **2007**, *111*, 5703−5711.

(15) Ghosh, N.; Cui, Q. pKa of residue 66 in Staphylococal nuclease. I. Insights from QM/MM simulations with conventional sampling. *J. Phys. Chem. B* **2008**, *112*, 8387−8397.

(16) Li, G.; Zhang, X.; Cui, Q. Free Energy Perturbation Calculations with Combined QM/MM Potentials Complications, Simplifications,

and Applications to Redox Potential Calculations. *J. Phys. Chem. B* **2003**, *107*, 8643−8653.

(17) Blumberger, J.; Sprik, M. Quantum versus classical electron transfer energy as reaction coordinate for the aqueous Ru2+/Ru3+ redox reaction. *Theor. Chem. Acc.* **2005**, *115*, 113−126.

(18) Borhani, D. W.; Shaw, D. E. The future of molecular dynamics simulations in drug discovery. *J. Comput.-Aided Mol. Des.* **2012**, *26*, 15−26.

(19) Mobley, D. L. Let's get honest about sampling. *J. Comput.-Aided Mol. Des.* **2012**, *26*, 93−95.

(20) Nicholls, A.; Mobley, D. L.; Guthrie, J. P.; Chodera, J. D.; Bayly, C. I.; Cooper, M. D.; Pande, V. S. Predicting small-molecule solvation free energies: An informal blind test for computational chemistry. *J. Med. Chem.* **2008**, *51*, 769−779.

(21) Guthrie, J. P. A Blind Challenge for Computational Solvation Free Energies: Introduction and Overview. *J. Phys. Chem. B* **2009**, *113*, 4501−4507.

(22) Geballe, M. T.; Skillman, A. G.; Nicholls, A.; Guthrie, J. P.; Taylor, P. J. The SAMPL2 blind prediction challenge: introduction and overview. *J. Comput.-Aided Mol. Des.* **2010**, *24*, 259−279.

(23) Muddana, H. S.; Varnado, C. D.; Bielawski, C. W.; Urbach, A. R.; Isaacs, L.; Geballe, M. T.; Gilson, M. K. Blind prediction of host-guest binding affinities: a new SAMPL3 challenge. *J. Comput.-Aided Mol. Des.* **2012**, *26*, 475−487.

(24) Klimovich, P. V.; Mobley, D. L. Predicting hydration free energies using all-atom molecular dynamics simulations and multiple starting conformations. *J. Comput.-Aided Mol. Des.* **2010**, *24*, 307−316.

(25) König, G.; Brooks, B. R. Predicting binding affinities of host-guest systems in the SAMPL3 blind challenge: the performance of relative free energy calculations. *J. Comput.-Aided Mol. Des.* **2012**, *26*, 543−550.

(26) Gallicchio, E.; Levy, R. M. Prediction of SAMPL3 host-guest affinities with the binding energy distribution analysis method (BEDAM). *J. Comput.-Aided Mol. Des.* **2012**, *26*, 505−516.

(27) Lawrenz, M.; Wereszczynski, J.; Ortiz-Sánchez, J. M.; Nichols, S. E.; McCammon, J. A. Thermodynamic integration to predict host-guest binding affinities. *J. Comput.-Aided Mol. Des.* **2012**, *26*, 569−576.

(28) Mobley, D. L.; Liu, S.; Cerutti, D. S.; Swope, W. C.; Rice, J. E. Alchemical prediction of hydration free energies for SAMPL. *J. Comput.-Aided Mol. Des.* **2012**, *26*, 551−562.

(29) Stanton, R. V.; Hartsough, D. S.; Merz, K. M. Calculation of solvation free energies using a density functional/molecular dynamics coupled potential. *J. Phys. Chem.* **1993**, *97*, 11868−11870.

(30) Reddy, M. R.; Singh, U. C.; Erion, M. D. Development of a quantum mechanics-based free-energy perturbation method: use in the calculation of relative solvation free energies. *J. Am. Chem. Soc.* **2004**, *126*, 6224−6225.

(31) Reddy, M. R.; Singh, U. C.; Erion, M. D. Ab initio quantum mechanics-based free energy perturbation method for calculating relative solvation free energies. *J. Comput. Chem.* **2007**, *28*, 491−494.

(32) Riccardi, D.; Schaefer, P.; Yang, Y.; Yu, H.; Ghosh, N.; Prat-Resina, X.; König, P.; Li, G.; Xu, D.; Guo, H.; Elstner, M.; Cui, Q. Development of effective quantum mechanical/molecular mechanical (QM/MM) methods for complex biological processes. *J. Phys. Chem. B* **2006**, *110*, 6458−6469.

(33) Yang, W.; Cui, Q.; Min, D.; Li, H. *QM/MM Alchemical Free Energy Simulations: Challenges and Recent Developments*; Annual Reports in Computational Chemistry; Elsevier: 2010; Vol. 6.

(34) Yang, W.; Bitetti-Putzer, R.; Karplus, M. Chaperoned alchemical free energy simulations: a general method for QM, MM, and QM/MM potentials. *J. Chem. Phys.* **2004**, *120*, 9450−9453.

(35) Min, D.; Chen, M.; Zheng, L.; Jin, Y.; Schwartz, M. A.; Sang, Q.-X. A.; Yang, W. Enhancing QM/MM molecular dynamics sampling in explicit environments via an orthogonal-space-random-walk-based strategy. *J. Phys. Chem. B* **2011**, *115*, 3924−3935.

(36) Min, D.; Zheng, L.; Harris, W.; Chen, M.; Lv, C.; Yang, W. Practically Efficient QM/MM Alchemical Free Energy Simulations: The Orthogonal Space Random Walk Strategy. *J. Chem. Theory Comput.* **2010**, *6*, 2253−2266.

(37) Kästner, J.; Senn, H.; Thiel, S.; Otte, N.; Thiel, W. QM/MM free-energy perturbation compared to thermodynamic integration and umbrella sampling: Application to an enzymatic reaction. *J. Chem. Theory Comput.* **2006**, *2*, 452−461.

(38) Polyak, I.; Benighaus, T.; Boulanger, E.; Thiel, W. Quantum mechanics/molecular mechanics dual Hamiltonian free energy perturbation. *J. Chem. Phys.* **2013**, *139*, 064105−064116.

(39) Senn, H. M.; Thiel, W. QM/MM methods for biomolecular systems. *Angew. Chem., Int. Ed.* **2009**, *48*, 1198−1229.

(40) Nam, K.; Gao, J.; York, D. M. An Efficient Linear-Scaling Ewald Method for Long-Range Electrostatic Interactions in Combined QM/MM Calculations. *J. Chem. Theory Comput.* **2005**, *1*, 2−13.

(41) Štrajbl, M.; Hong, G.; Warshel, A. Ab Initio QM/MM Simulation with Proper Sampling: "First Principle" Calculations of the Free Energy of the Autodissociation of Water in Aqueous Solution. *J. Phys. Chem. B* **2002**, *106*, 13333−13343.

(42) Plotnikov, N. V.; Kamerlin, S. C. L.; Warshel, A. Paradynamics: an effective and reliable model for ab initio QM/MM free-energy calculations and related tasks. *J. Phys. Chem. B* **2011**, *115*, 7950−7962.

(43) Gao, J.; Xia, X. A priori evaluation of aqueous polarization effects through Monte Carlo QM-MM simulations. *Science* **1992**, *258*, 631−635.

(44) Gao, J.; Luque, F. J.; Orozco, M. Induced dipole moment and atomic charges based on average electrostatic potentials in aqueous solution. *J. Chem. Phys.* **1993**, *98*, 2975−2982.

(45) Luzhkov, V.; Warshel, A. Microscopic models for quantum mechanical calculations of chemical processes in solutions: LD/AMPAC and SCAAS/AMPAC calculations of solvation energies. *J. Comput. Chem.* **1992**, *13*, 199−213.

(46) Wesolowski, T.; Warshel, A. Ab Initio Free Energy Perturbation Calculations of Solvation Free Energy Using the Frozen Density Functional Approach. *J. Phys. Chem.* **1994**, *98*, 5183−5187.

(47) Gao, J.; Freindorf, M. Hybrid ab Initio QM/MM Simulation of N -Methylacetamide in Aqueous Solution. *J. Phys. Chem. A* **1997**, *101*, 3182−3188.

(48) Kollman, P. Free energy calculations: Applications to chemical and biochemical phenomena. *Chem. Rev.* **1993**, *93*, 2395−2417.

(49) Chandrasekhar, J.; Smith, S. F.; Jorgensen, W. L. SN2 reaction profiles in the gas phase and aqueous solution. *J. Am. Chem. Soc.* **1984**, *106*, 3049−3050.

(50) Chandrasekhar, J.; Smith, S. F.; Jorgensen, W. L. Theoretical examination of the SN2 reaction involving chloride ion and methyl chloride in the gas phase and aqueous solution. *J. Am. Chem. Soc.* **1985**, *107*, 154−163.

(51) Thiel, W.; Voityuk, A. A. Extension of MNDO to d Orbitals: Parameters and Results for the Second-Row Elements and for the Zinc Group. *J. Phys. Chem.* **1996**, *100*, 616−626.

(52) Das, D.; Eurenius, K. P.; Billings, E. M.; Sherwood, P.; Chatfield, D. C.; Hodoscek, M.; Brooks, B. R. Optimization of quantum mechanical molecular mechanical partitioning schemes: Gaussian delocalization of molecular mechanical charges and the double link atom method. *J. Chem. Phys.* **2002**, *117*, 10534−10547.

(53) Lyne, P. D.; Hodoscek, M.; Karplus, M. A Hybrid QM-MM Potential Employing Hartree-Fock or Density Functional Methods in the Quantum Region. *J. Phys. Chem. A* **1999**, *103*, 3462−3471.

(54) Luque, F. J.; Reuter, N.; Cartier, A.; Ruiz-López, M. F. Calibration of the Quantum/Classical Hamiltonian in Semiempirical QM/MM AM1 and PM3 Methods. *J. Phys. Chem. A* **2000**, *104*, 10923−10931.

(55) Tuttle, T.; Thiel, W. OMx-D: semiempirical methods with orthogonalization and dispersion corrections. Implementation and biochemical application. *Phys. Chem. Chem. Phys.* **2008**, *10*, 2159−2166.

(56) Repasky, M. P.; Chandrasekhar, J.; Jorgensen, W. L. PDDG/PM3 and PDDG/MNDO: Improved semiempirical methods. *J. Comput. Chem.* **2002**, *23*, 1601−1622.

(57) Elstner, M.; Porezag, D.; Jungnickel, G.; Elsner, J.; Haugk, M.; Frauenheim, T.; Suhai, S.; Seifert, G. Self-consistent-charge density-

functional tight-binding method for simulations of complex materials properties. *Phys. Rev. B* **1998**, *58*, 7260−7268.

(58) Lonsdale, R.; Hoyle, S.; Grey, D. T.; Ridder, L.; Mulholland, A. J. Determinants of reactivity and selectivity in soluble epoxide hydrolase from quantum mechanics/molecular mechanics modeling. *Biochemistry* **2012**, *51*, 1774−1786.

(59) Bowman, A. L.; Grant, I. M.; Mulholland, A. J. QM/MM simulations predict a covalent intermediate in the hen egg white lysozyme reaction with its natural substrate. *Chem. Commun.* **2008**, *37*, 4425−4427.

(60) Claeyssens, F.; Harvey, J. N.; Manby, F. R.; Mata, R. A.; Mulholland, A. J.; Ranaghan, K. E.; Schütz, M.; Thiel, S.; Thiel, W.; Werner, H.-J. High-accuracy computation of reaction barriers in enzymes. *Angew. Chem., Int. Ed.* **2006**, *45*, 6856−6859.

(61) Lonsdale, R.; Harvey, J. N.; Mulholland, A. J. Inclusion of Dispersion Effects Significantly Improves Accuracy of Calculated Reaction Barriers for Cytochrome P450 Catalyzed Reactions. *Phys. Chem. Lett.* **2010**, *1*, 3232−3237.

(62) Li, H.; Yang, W. Sampling enhancement for the quantum mechanical potential based molecular dynamics simulations: A general algorithm and its extension for free energy calculation on rugged energy surface. *J. Chem. Phys.* **2007**, *126*, 114104.

(63) Woods, C. J.; Manby, F. R.; Mulholland, A. J. An efficient method for the calculation of quantum mechanics/molecular mechanics free energies. *J. Chem. Phys.* **2008**, *128*, 014109.

(64) Rod, T. H.; Ryde, U. Accurate QM/MM Free Energy Calculations of Enzyme Reactions: Methylation by Catechol O-Methyltransferase. *J. Chem. Theory Comput.* **2005**, *1*, 1240−1251.

(65) Rod, T.; Ryde, U. Quantum Mechanical Free Energy Barrier for an Enzymatic Reaction. *Phys. Rev. Lett.* **2005**, *94*, 138302.

(66) Heimdal, J.; Ryde, U. Convergence of QM/MM free-energy perturbations based on molecular-mechanics or semiempirical simulations. *Phys. Chem. Chem. Phys.* **2012**, *14*, 12592−12604.

(67) Hu, H.; Lu, Z.; Yang, W. QM/MM Minimum Free Energy Path: Methodology and Application to Triosephosphate Isomerase. *J. Chem. Theory Comput.* **2007**, *3*, 390−406.

(68) Zeng, X.; Hu, H.; Hu, X.; Cohen, A. J.; Yang, W. Ab initio quantum mechanical/molecular mechanical simulation of electron transfer process: fractional electron approach. *J. Chem. Phys.* **2008**, *128*, 124510.

(69) Hu, H.; Lu, Z.; Parks, J. M.; Burger, S. K.; Yang, W. Quantum mechanics/molecular mechanics minimum free-energy path for accurate reaction energetics in solution and enzymes: sequential sampling and optimization on the potential of mean force surface. *J. Chem. Phys.* **2008**, *128*, 034105.

(70) Hu, H.; Yang, W. Elucidating solvent contributions to solution reactions with ab initio QM/MM methods. *J. Phys. Chem. B* **2010**, *114*, 2755−2759.

(71) Zacharias, M.; Straatsma, T. P.; McCammon, J. A. Separation-Shifted Scaling, a New Scaling Method for Lennard-Jones Interactions in Thermodynamic Integration. *J. Chem. Phys.* **1994**, *100*, 9025−9031.

(72) Beutler, T. C.; Mark, A. E.; van Schaik, R. C.; Gerber, P. R.; van Gunsteren, W. F. Avoiding Singularities and Numerical Instabilities in Free Energy Calculations Based on Molecular Simulations. *Chem. Phys. Lett.* **1994**, *222*, 529−539.

(73) Zwanzig, R. W. High-Temperature Equation Of State By A Perturbation Method. 1. Nonpolar Gases. *J. Chem. Phys.* **1954**, *22*, 1420−1426.

(74) Zhang, Y.; Liu, H.; Yang, W. Free energy calculation on enzyme reactions with an efficient iterative procedure to determine minimum energy paths on a combined ab initio QM/MM potential energy surface. *J. Chem. Phys.* **2000**, *112*, 3483−3492.

(75) Mart, S.; Moliner, V.; Tuñón, I.; Williams, I. H. Computing kinetic isotope effects for chorismate mutase with high accuracy. A new DFT/MM strategy. *J. Phys. Chem. B* **2005**, *109*, 3707−3710.

(76) Martí, S.; Moliner, V.; Tuñón, I. Improving the QM/MM Description of Chemical Processes: A Dual Level Strategy to Explore the Potential Energy Surface in Very Large Systems. *J. Chem. Theory Comput.* **2005**, *1*, 1008−1016.

(77) Bentzien, J.; Muller, R. P.; Florián, J.; Warshel, A. Hybrid ab Initio Quantum Mechanics/Molecular Mechanics Calculations of Free Energy Surfaces for Enzymatic Reactions: The Nucleophilic Attack in Subtilisin. *J. Phys. Chem. A* **1998**, *102*, 2293−2301.

(78) Frushicheva, M. P.; Warshel, A. Towards quantitative computer-aided studies of enzymatic enantioselectivity: the case of Candida antarctica lipase A. *ChemBioChem* **2012**, *13*, 215−223.

(79) Heimdal, J.; Ryde, U. Convergence of QM/MM free-energy perturbations based on molecular-mechanics or semiempirical simulations. *Phys. Chem. Chem. Phys.* **2012**, *14*, 12592−12604.

(80) Fox, S. J.; Pittock, C.; Tautermann, C. S.; Fox, T.; Christ, C.; Malcolm, N. O. J.; Essex, J. W.; Skylaris, C.-K. Free energies of binding from large-scale first-principles quantum mechanical calculations: application to ligand hydration energies. *J. Phys. Chem. B* **2013**, *117*, 9478−9485.

(81) Beierlein, F. R.; Michel, J.; Essex, J. W. A Simple QM/MM Approach for Capturing Polarization Effects in Protein-Ligand Binding Free Energy Calculations. *J. Phys. Chem. B* **2011**, *115*, 4911−4926.

(82) Lu, N.; Kofke, D. A.; Woolf, T. B. Improving the efficiency and reliability of free energy perturbation calculations using overlap sampling methods. *J. Comput. Chem.* **2004**, *25*, 28−40.

(83) Shirts, M. R.; Pande, V. S. Comparison of efficiency and bias of free energies computed by exponential averaging, the Bennett acceptance ratio, and thermodynamic integration. *J. Chem. Phys.* **2005**, *122*, 144107-1−144107-16.

(84) Bruckner, S.; Boresch, S. Efficiency of Alchemical Free Energy Simulations I: Practical Comparison of the Exponential Formula, Thermodynamic Integration and Bennett's Acceptance Ratio Method. *J. Comput. Chem.* **2011**, *32*, 1303−1319.

(85) Bruckner, S.; Boresch, S. Efficiency of Alchemical Free Energy Simulations II: Improvements for Thermodynamic Integration. *J. Comput. Chem.* **2011**, *32*, 1320−1333.

(86) Bennett, C. H. Efficient Estimation of Free Energy Differences from Monte Carlo Data. *J. Comput. Phys.* **1976**, *22*, 245−268.

(87) Kirkwood, J. G. Statistical Mechanics of Fluid Mixtures. *J. Chem. Phys.* **1935**, *3*, 300−313.

(88) König, G.; Bruckner, S.; Boresch, S. Unorthodox Uses of Bennett's Acceptance Ratio Method. *J. Comput. Chem.* **2009**, *30*, 1712−1718.

(89) Pohorille, A.; Jarzynski, C.; Chipot, C. Good Practices in Free-Energy Calculations. *J. Phys. Chem. B* **2010**, *114*, 10235−10253.

(90) Rosta, E.; Klähn, M.; Warshel, A. Towards accurate ab initio QM/MM calculations of free-energy profiles of enzymatic reactions. *J. Phys. Chem. B* **2006**, *110*, 2934−2941.

(91) König, G.; Boresch, S. Non-Boltzmann Sampling and Bennett's Acceptance Ratio Method: How to Profit from Bending the Rules. *J. Comput. Chem.* **2011**, *32*, 1082−1090.

(92) Zwanzig, R. W. High-Temperature Equation of State by a Perturbation Method. I. Nonpolar Gases. *J. Chem. Phys.* **1954**, *22*, 1420−1426.

(93) Jorgensen, W. L.; Thomas, L. L. Perspective on Free-Energy Perturbation Calculations for Chemical Equilibria. *J. Chem. Theory Comput.* **2008**, *4*, 869−876.

(94) Shirts, M. R.; Pitera, J. W.; Swope, W. C.; Pande, V. S. Extremely precise free energy calculations of amino acid side chain analogs: Comparison of common molecular mechanics force fields for proteins. *J. Chem. Phys.* **2003**, *119*, 5740−5761.

(95) Torrie, G. M.; Valleau, J. P. Non-physical sampling distributions in Monte-Carlo free energy estimation - umbrella sampling. *J. Comput. Phys.* **1977**, *23*, 187−199.

(96) Wereszczynski, J.; McCammon, J. A. Using Selectively Applied Accelerated Molecular Dynamics to Enhance Free Energy Calculations. *J. Chem. Theory Comput.* **2010**, *6*, 3285−3292.

(97) Straatsma, T. P.; McCammon, J. A. Treatment of rotational isomeric states. III. The use of biasing potentials. *J. Chem. Phys.* **1994**, *101*, 5032−5039.

(98) Leitgeb, M.; Schröder, C.; Boresch, S. Alchemical Free Energy Calculations and Multiple Conformational Substates. *J. Chem. Phys.* **2005**, *122*, 084109.

(99) Mobley, D. L.; Dill, K. A.; Chodera, J. D. Treating Entropy and Conformational Changes in Implicit Solvent Simulations of Small Molecules. *J. Phys. Chem. B* **2008**, *112*, 938−946.

(100) Brooks, B.; Brooks, C., III; Mackerell, A., Jr.; Nilsson, L.; Petrella, R.; Roux, B.; Won, Y.; Archontis, G.; Bartels, C.; Boresch, S.; Caflisch, A.; Caves, L.; Cui, Q.; Dinner, A.; Feig, M.; Fischer, S.; Gao, J.; Hodoscek, M.; Im, W.; Kuczera, K.; Lazaridis, T.; Ma, J.; Ovchinnikov, V.; Paci, E.; Pastor, R.; Post, C.; Pu, J.; Schaefer, M.; Tidor, B.; Venable, R.; Woodcock, H.; Wu, X.; Yang, W.; York, D.; Karplus, M. CHARMM: The Biomolecular Simulation Program. *J. Comput. Chem.* **2009**, *30*, 1545−1614.

(101) Brooks, B. R.; Bruccoleri, R. E.; Olafson, B. D.; States, D. J.; Swaminathan, S.; Karplus, M. CHARMM: A program for macro-molecular energy, minimization and dynamics calculations. *J. Comput. Chem.* **1983**, *4*, 187−217.

(102) MacKerell, A. D., Jr.; Bashford, D.; Bellott, M.; Dunbrack, R. L., Jr.; Evanseck, J. D.; Field, M. J.; Fischer, S.; Gao, J.; Guo, H.; Ha, S.; Joseph-McCarthy, D.; Kuchnir, L.; Kuczera, K.; Lau, F. T. K.; Mattos, C.; Michnick, S.; Ngo, T.; Nguyen, D. T.; Prodhom, B.; Reiher, W. E., III; Roux, B.; Schlenkrich, M.; Smith, J.; Stote, R.; Straub, J.; Watanabe, M.; Wiorkiewicz-Kuczera, J.; Yin, D.; Karplus, M. All-atom empirical potential for molecular modeling and dynamics studies of protein. *J. Phys. Chem. B* **1998**, *102*, 3586−3616.

(103) Shao, Y.; Molnar, L. F.; Jung, Y.; Kussmann, J.; Ochsenfeld, C.; Brown, S. T.; Gilbert, A. T. B.; Slipchenko, L. V.; Levchenko, S. V.; O'Neill, D. P.; DiStasio, R. A., Jr.; Lochan, R. C.; Wang, T.; Beran, G. J. O.; Besley, N. A.; Herbert, J. M.; Lin, C. Y.; Van Voorhis, T.; Chien, S. H.; Sodt, A.; Steele, R. P.; Rassolov, V. A.; Maslen, P. E.; Korambath, P. P.; Adamson, R. D.; Austin, B.; Baker, J.; Byrd, E. F. C.; Dachsel, H.; Doerksen, R. J.; Dreuw, A.; Dunietz, B. D.; Dutoi, A. D.; Furlani, T. R.; Gwaltney, S. R.; Heyden, A.; Hirata, S.; Hsu, C.-P.; Kedziora, G.; Khalliulin, R. Z.; Klunzinger, P.; Lee, A. M.; Lee, M. S.; Liang, W.; Lotan, I.; Nair, N.; Peters, B.; Proynov, E. I.; Pieniazek, P. A.; Rhee, Y. M.; Ritchie, J.; Rosta, E.; Sherrill, C. D.; Simmonett, A. C.; Subotnik, J. E.; Woodcock, H. L., III; Zhang, W.; Bell, A. T.; Chakraborty, A. K.; Chipman, D. M.; Keil, F. J.; Warshel, A.; Hehre, W. J.; Schaefer, H. F., III; Kong, J.; Krylov, A. I.; Gill, P. M. W.; Head-Gordon, M. Advances in methods and algorithms in a modern quantum chemistry program package. *Phys. Chem. Chem. Phys.* **2006**, *8*, 3172−3191.

(104) Woodcock, H. L., III; Hodoscek, M.; Gilbert, A. T. B.; Gill, P. M. W.; Schaefer, H. F., III; Brooks, B. R. Interfacing Q-chem and CHARMM to perform QM/MM reaction path calculations. *J. Comput. Chem.* **2007**, *28*, 1485−1502.

(105) Pearlman, D. A. A Comparison of Alternative Approaches to Free Energy Calculations. *J. Phys. Chem.* **1994**, *98*, 1487−1493.

(106) Boresch, S.; Karplus, M. The Role of Bonded Terms in Free Energy Simulations: 1. Theoretical Analysis. *J. Phys. Chem. A* **1999**, *103*, 103−118.

(107) Tembe, B. L.; McCammon, J. A. Ligand-receptor interactions. *Comput. Chem.* **1984**, *8*, 281−283.

(108) Woodcock, H. L.; Miller, B. T.; Hodoscek, M.; Okur, A.; Larkin, J. D.; Ponder, J. W.; Brooks, B. R. MSCALE: A General Utility for Multiscale Modeling. *J. Chem. Theory Comput.* **2011**, *7*, 1208−1219.

(109) Boresch, S.; Karplus, M. The Role of Bonded Terms in Free Energy Simulations. 2. Calculation of Their Influence on Free Energy Differences of Solvation. *J. Phys. Chem. A* **1999**, *103*, 119−136.

(110) Hoover, W. G. Canonical Dynamics: Equilibrium Phase-Space Distributions. *Phys. Rev. A* **1985**, *31*, 1695−1697.

(111) Essmann, U.; Perera, L.; Berkowitz, M. L.; Darden, T.; Lee, H.; Pedersen, L. G. A smooth particle mesh Ewald method. *J. Chem. Phys.* **1995**, *103*, 8577−8593.

(112) Lee, M. S.; Feig, M.; Salsbury, F. R.; Brooks, C. L., III. New analytic approximation to the standard molecular volume definition and its application to generalized born calculations. *J. Comput. Chem.* **2003**, *23*, 1348−1356.

(113) Zhao, Y.; Truhlar, D. G. The M06 suite of density functionals for main group thermochemistry, thermochemical kinetics, non-covalent interactions, excited states, and transition elements: two new functionals and systematic testing of four M06-class functionals and 12 other function. *Theor. Chem. Acc.* **2007**, *120*, 215−241.

(114) Becke, A. D. A new mixing of Hartree-Fock and local-density-functional theories. *J. Chem. Phys.* **1993**, *98*, 1372−1377.

(115) Lee, C.; Yang, W.; Parr, R. G. Development of the Colle-Salvetti correlation-energy formula into a functional of the electron density. *Phys. Rev. B* **1988**, *37*, 785−789.

(116) Marenich, A. V.; Cramer, C. J.; Truhlar, D. G. Universal solvation model based on solute electron density and on a continuum model of the solvent defined by the bulk dielectric constant and atomic surface tensions. *J. Phys. Chem. B* **2009**, *113*, 6378−6396.

(117) Gordon, M. S.; Schmidt, M. W. In *Theory and Applications of Computational Chemistry: the first forty years*; Dykstra, C. E., Frenking, G., Kim, K. S., Scuseria, G. E., Eds.; Elsevier: Amsterdam, 2005; pp 1167−1189.

(118) Marenich, A. V.; Cramer, C. J.; Truhlar, D. G. Universal Solvation Model Based on the Generalized Born Approximation with Asymmetric Descreening. *J. Chem. Theory Comput.* **2009**, *5*, 2447−2464.

(119) Marenich, A. V.; Cramer, C. J.; Truhlar, D. G. Generalized Born Solvation Model SM12. *J. Chem. Theory Comput.* **2013**, *9*, 609−620.

(120) Villa, A.; Mark, A. E. Calculation of the free energy of solvation for neutral analogs of amino acid side chains. *J. Comput. Chem.* **2002**, *23*, 548−553.

(121) Deng, Y. Q.; Roux, B. Hydration of amino acid side chains: Nonpolar and electrostatic contributions calculated from staged molecular dynamics free energy simulations with explicit water molecules. *J. Phys. Chem. B* **2004**, *108*, 16567−16576.

(122) Vanommeslaeghe, K.; Hatcher, E.; Acharya, C.; Kundu, S.; Zhong, S.; Shim, J.; Darian, E.; Guvench, O.; Lopes, P.; Vorobyov, I.; Mackerell, A. D. CHARMM general force field: A force field for drug-like molecules compatible with the CHARMM all-atom additive biological force fields. *J. Comput. Chem.* **2010**, *31*, 671−690.

(123) Best, R. B.; Zhu, X.; Shim, J.; Lopes, P. E. M.; Mittal, J.; Feig, M.; MacKerell, A. D. Optimization of the Additive CHARMM All-Atom Protein Force Field Targeting Improved Sampling of the Backbone Φ, Ψ and Side-Chain χ_1 and χ_2 Dihedral Angles. *J. Chem. Theory Comput.* **2012**, *8*, 3257−3273.

(124) Beveridge, D. L.; DiCapua, F. M. In *Computer Simulation of Biomolecular Systems*; van Gunsteren, W. F., Weiner, P. K., Eds.; ESCOM Science: Leiden, 1989; pp 1−26.

(125) Ben-Naim, A.; Marcus, Y. J. Solvation thermodynamics of nonionic solutes. *J. Chem. Phys.* **1984**, *81*, 2016−2027.

(126) Lin, C. Y.; Gilbert, A. T. B.; Gill, P. M. W. Calculating molecular vibrational spectra beyond the harmonic approximation. *Theor. Chem. Acc.* **2007**, *120*, 23−35.

(127) Nicholls, A.; Mobley, D. L.; Guthrie, J. P.; Chodera, J. D.; Bayly, C. I.; Cooper, M. D.; Pande, V. S. Predicting Small-Molecule Solvation Free Energies: An Informal Blind Test for Computational Chemistry. *J. Med. Chem.* **2008**, *51*, 769−779.

(128) Mobley, D. L.; Bayly, C. I.; Cooper, M. D.; Shirts, M. R.; Dill, K. A. Small Molecule Hydration Free Energies in Explicit Solvent: An Extensive Test of Fixed-Charge Atomistic Simulations. *J. Chem. Theory Comput.* **2009**, *5*, 350−358.

(129) Mobley, D. L.; Liu, S.; Cerutti, D. S.; Swope, W. C.; Rice, J. E. Alchemical prediction of hydration free energies for SAMPL. *J. Comput.-Aided Mol. Des.* **2012**, *26*, 551−562.